Minimal normal-form method for discrete maps

S. R. Mane and W. T. Weng
Brookhaven National Laboratory, Upton, New York 11973
(Received 4 December 1992; revised manuscript received 19 February 1993)

Normal-form methods for solving nonlinear differential equations are reviewed and the comparative merits of three methods are evaluated. The method of minimal normal forms is then extended to apply to the evaluation of discrete maps of an accelerator or storage ring. Such an extension, as suggested in this paper, is more suited for accelerator-based applications than a formulation utilizing continuous differential equations. A computer code has been generated to implement systematically various normal-form formulations for maps in two-dimensional phase space. Specific examples of quadratic and cubic nonlinear fields were used and solved by the method developed. The minimal normal-form method shown here gives good results using relatively-low-order expansions.

PACS number(s): 41.85.−p, 29.27.Bd, 29.20.Dh

I. INTRODUCTION

It is relatively easy and straightforward to find solutions of accelerator lattice design for a linear system [1]. Once the nonlinear elements are introduced, no preferred method has been found. Lately, one-turn maps [2] have been suggested as a useful tool for embodying all perturbations in an accelerator and hence a testing bed for evaluating the comparative merits of various approaches. A good one-turn map representation of an accelerator can provide all necessary information for the lattice description and hopefully also facilitate the evaluation of the short-term stability and dynamic aperture of the accelerator or storage ring.

Motivated by the successful and apparently superior performance of the method of minimal normal forms [3] in solving ordinary nonlinear differential equations, this report is a first attempt to apply the same method to the evaluation of maps suitable for accelerator design. A good general discussion of normal forms is given in Ref. [4]. An example of the application of normal-form techniques, for the (large hadron collider) (LHC) at CERN (but not using minimal normal forms), is given in Ref. [5], demonstrating the usefulness of normal forms. The method of averaging [6] is also broadly similar in spirit to the techniques discussed in this paper. Our goal is to find a rapidly convergent method that can provide basic reliable particle behavior and lattice information in a few terms.

In this context, normal-form methods for solving differential equations are first reviewed briefly and evidence of the superiority of the minimal normal-form (MNF) approach is demonstrated. Then the methods are extended to the evaluation of one-turn maps for accelerators. Both analytical and numerical methods of calculating the free functions in the normal-form transformations are presented and applied to quadratic, cubic, and combined perturbations. Unfortunately, the superiority of the MNF method is not self-evident for the evaluation of maps. The underlying reasons for the average performance will be investigated and methods for improvements explored in a future study.

II. REVIEW OF FORMALISM

A. Formulation of method for differential equations

The minimal normal-form method as applied to differential equations will be introduced below. This will also serve the purpose of defining some notations and preparing the groundwork for an extension of the method to treat discrete maps. The notation follows that of Ref. [3], which also gives a description of the method. However, their presentation (which treats only differential equations) is not cast in a form directly useful to the development below.

Consider a dynamical system describable by a canonically conjugate (coordinate, momentum) pair (x,p), with $z=x+ip$, which executes a harmonic oscillation with a nonlinear autonomous perturbation

$$\dot{z}=-i\mu z+\sum_{k=1}^{\infty}\epsilon^k Z_k(z,z^*)\ , \tag{2.1}$$

where the frequency is μ, ϵ is the small parameter of the perturbation expansion, and the Z_k are *homogeneous* polynomials of degree $k+1$ in z and z^*, given by

$$Z_k=\sum_{(p+q=k+1)} Z_{pq}z^p z^{*q}\ . \tag{2.2}$$

The above equation is now solved by the use of a near-identity transformation to a normal-form variable u via

$$z=u+\sum_{k=1}^{\infty}\epsilon^k T_k(u,u^*)\ , \tag{2.3}$$

with homogeneous polynomials

$$T_k=\sum_{(p+q=k+1)} T_{pq}u^p u^{*q}\ , \tag{2.4}$$

which are to be determined. Let the resulting equation of motion for u be expressed as

$$\dot{u}=-i\Omega(u,u^*)u\ , \tag{2.5}$$

where it is anticipated that the motion of u will be a rota-

tion in phase space. To make u a normal-form variable, in which case Eq. (2.3) is called a normalizing transformation, the functions T_k are chosen so that Ω will be a function of uu^* only,

$$\dot{u}=-i\Omega(uu^*)u \ , \qquad \Omega=\mu+i\sum_k \epsilon^{2k}\tilde{U}_{2k}(uu^*)^k \ . \tag{2.6}$$

The solution for u will have the form $u=\rho e^{-i\psi}$, where ρ is constant and

$$\psi=\psi_0+\Omega(\rho^2)t \ . \tag{2.7}$$

This prescription uniquely determines all of the coefficients T_{pq} except those for which $p=q+1$, i.e., the coefficients of $u(uu^*)^p$, $p=1,2,\ldots$. In other words, the above prescription insures that the motion of u is an amplitude-dependent phase-space rotation, which is the well-known behavior of normal forms, but it does not fix the values of the tune-shift coefficients $\tilde{U}_{2k}$ (tune being the dimensionless frequency). The coefficients $T_{p+1,p}$ will be called "free terms" or "free functions." An extra criterion is required to fix them, which will also set the values of the tune-shift terms.

It is at this point that the various methods of calculating normal forms differ from each other. The "simplest" choice is to put all the free functions to zero. This will fix the terms $\tilde{U}_{2k}$ in Eq. (2.6) uniquely, and yield a well-defined infinite series of amplitude-dependent frequency shifts. However, it is not necessary to set the free functions to zero. The relation between the Poisson brackets $[z,z^*]$ and $[u,u^*]$ is of the form

$$[z,z^*]=[u,u^*]\left\{1+\sum_{k=0}^{\infty}\epsilon^{2k}\tilde{P}_{2k}(uu^*)^k\right\} , \tag{2.8}$$

where the $\tilde{P}_{2k}$ obviously depend on the coefficients T_{pq}. Choosing the free functions to cancel all the P_{2k} makes the near-identity transformation in Eq. (2.3) a canonical transformation. This requires nonzero values for the free functions; it also leads to different values for the amplitude-dependent frequency-shift terms $\tilde{U}_{2k}$ in Eq. (2.6). The choice of canonical transformations is often automatic in the accelerator-physics literature, since there is a well-developed theory of such transformations, e.g., the use of generating functions. The present formulation displays the range of some of the other alternatives available for obtaining normal forms.

In this context, the minimal normal-form method provides another prescription for choosing the values of the free functions. Instead of cancelling the Poisson-bracket terms $\tilde{P}_{2k}$, one chooses the free functions to cancel out the tune-shift corrections, the $\tilde{U}_{2k}$'s. In practice, one finds that the free term of order $2k$, viz., $T_{k+1\,k}$, can be used to cancel the tune-shift term of order $2k+2$, $\tilde{U}_{2k+2}$. The first term $\tilde{U}_2$ thus cannot be canceled, which therefore leaves

$$\dot{u}=-i\mu u+\epsilon^2\tilde{U}_2u^3u^{*2} \ . \tag{2.9}$$

Hence the minimal normal-form method also leads to nonzero values for the free functions, but reduces the infinite series of higher-order corrections to the normal form to only one term: This explains the name "minimal" normal form. The resulting transformation from the original coordinates to the normal form is not canonical. It will be shown below, for various models, that the normalizing transformation in Eq. (2.3) converges much more rapidly if one uses the minimal normal form rather than a canonical transformation, or the "free function equal to zero" choice.

B. Treatment of discrete maps

The method of minimal normal forms will now be extended to treat discrete maps, as opposed to differential equations as in the previously published literature [3]. As explained above, such a reformulation is more suited to accelerator-based applications. Only a two-dimensional phase space will be treated here. We again define $z=x+ip$, where (x,p) is the coordinate-momentum pair, and suppose that the map equation relating one turn to the next is

$$z_{n+1}=\lambda z_n+\sum_{k=1}^{\infty}\epsilon^k Z_k(z_n,z_n^*) \ , \tag{2.10}$$

where n is the turn number, $\lambda=e^{-i\mu}$, and the Z_k are again homogeneous polynomials of degree $k+1$ in z and z^*:

$$Z_k=\sum_{p+q=k+1}Z_{pq}z^pz^{*q} \ . \tag{2.11}$$

The near-identity transformation to the normal-form variable u is given by

$$z=u+\sum_{k=1}^{\infty}\epsilon^kT_k(u,u^*) \ , \tag{2.12}$$

with homogeneous polynomials T_k of degree $k+1$ in u and u^*:

$$T_k=\sum_{(p+q=k+1)}T_{pq}u^pu^{*q} \ . \tag{2.13}$$

This form of the near-identity transformation is essentially the same as that of Scandale, Schmidt, and Todesco [5], who express the homogeneous polynomials as Φ_s (summing over s), rather than T_k (summing over k). As in Ref. [5], we consider only the nonresonant normal form in this paper. Unlike them, we aim to terminate the tune-shift corrections at a finite order. Analogous to the case of differential equations, the T_{pq} are chosen so that the map for u will have the general form

$$u_{n+1}=e^{-i\Omega(u_nu_n^*)}u_n=u_n\lambda\left[1+\sum_{k=1}^{\infty}\epsilon^{2k}\tilde{U}_{2k}(u_nu_n^*)^k\right] , \tag{2.14}$$

where Ω consists of a sum of amplitude-dependent tune shifts and the minimal normal-form procedure is to choose the free functions to terminate the series for Ω at a finite order. *Unlike* the case with differential equations, however, the terms in Ω are not simply the $\tilde{U}_{2k}$; hence,

one *cannot* terminate the series for the tune shifts in Ω by setting the $\tilde{U}_{2k}$ to zero beyond $O(\epsilon^2)$. Instead, the free function $T_{k+1\,k}$ is chosen so that $\tilde{U}_{2k}/\lambda=(\tilde{U}_2/\lambda)^k/k!$. This then yields the map

$$u_{n+1}=\lambda u_n\left[1+\sum_k \frac{\epsilon^{2k}}{k!}\left[\frac{\tilde{U}_{2k}}{\lambda}\right]^k (uu^*)^k\right]$$
$$=\lambda u_n \exp[\epsilon^2(\tilde{U}_2/\lambda)uu^*] , \tag{2.15}$$

$$\Omega=\mu+i\epsilon^2(\tilde{U}_2/\lambda)\rho^2 , \tag{2.16}$$

i.e., a single higher-order exponent. The solution for u_n is again $\rho e^{-i\psi_n}$, where ρ is constant and

$$\psi_n=\psi_0+n\Omega(\rho^2) . \tag{2.17}$$

This is our generalization of Eq. (2.9) of the minimal normal-form condition as applied to maps. As in the case of differential equations, setting all the free functions to zero would require less effort in calculating the T_{pq} coefficients, but would yield an infinite series of amplitude-dependent tune-shift corrections:

$$\Omega=\mu+\epsilon^2\mu'\rho^2+\epsilon^4\mu''\rho^4+\cdots , \tag{2.18}$$

while a canonical transformation would yield both nonzero free functions and an infinite series of amplitude-dependent tune-shift corrections.

An obvious question is whether or not there is enough freedom to choose the free functions to cancel the higher-order tune-shift terms to obtain the minimal normal form as described above. An elegant proof of the existence of the minimal normal form has been supplied by Forest [7], using map-based techniques and the Dragt-Finn notation [8,9]. The proof therefore also applies automatically to differential equations. First, the original map is expressed in the form

$$z_{n+1}=\mathcal{M}z_n . \tag{2.19}$$

Using canonical transformations, the map $\mathcal{M}$ can be brought to normal form, say, $\mathcal{N}$, via a transformation $\mathcal{A}$:

$$\mathcal{M}=\mathcal{A}^{-1}\mathcal{N}\mathcal{A} . \tag{2.20}$$

It is well known that this normalization can be carried out, in a sufficiently small domain around the origin, for an origin-preserving map. There is some freedom in choosing $\mathcal{A}$, which can be explicitly expressed by noting that one can put $\mathcal{A}\rightarrow\mathcal{N}_1\mathcal{A}$, where $\mathcal{N}_1$ is an arbitrary amplitude-dependent rotation map, and

$$\mathcal{M}=\mathcal{A}^{-1}\mathcal{N}_1^{-1}\mathcal{N}\mathcal{N}_1\mathcal{A} , \tag{2.21}$$

because $\{\mathcal{N},\mathcal{N}_1\}=0$ by definition. The map $\mathcal{N}$ is an amplitude-dependent rotation, viz.,

$$\mathcal{N}=\exp\left[:\int_0^J -\mu(J')dJ':\right] , \tag{2.22}$$

where the colons indicate the Poisson-bracket operator, using Dragt-Finn notation [8],

$$:f:g=\{f,g\} , \tag{2.23}$$

and J is the invariant action, and $J=\rho^2/2$ for a canonical transformation. The tune shift has the form

$$\mu(J)=\mu+2\mu'J+\Gamma(J) , \tag{2.24}$$

where $\Gamma(J)$ is a shorthand for all the higher-order terms, and we have put $\epsilon=1$ in this derivation, without loss of generality. To convert the map to minimal normal form, we define

$$J_{\mathrm{MNF}}=J+\Gamma(J)/(2\mu') . \tag{2.25}$$

The tune-shift then becomes

$$\mu(J_{\mathrm{MNF}})=\mu+2\mu'J_{\mathrm{MNF}} , \tag{2.26}$$

i.e., a finite sum. Since J_{MNF} is a near-identity Taylor expansion in J, it can be inverted (at least in a domain close to the origin), so that one can express J as a function of J_{MNF}, and thereby obtain a map $\mathcal{B}=\mathcal{B}(J_{\mathrm{MNF}},\psi)$, where ψ is the angle variable, and write

$$\mathcal{M}=\mathcal{B}^{-1}\mathcal{N}_{\mathrm{MNF}}\mathcal{B} . \tag{2.27}$$

The map $\mathcal{B}$ is the normalizing transformation of the minimal normal form, and $\mathcal{N}_{\mathrm{MNF}}$ is the corresponding normalized map. Hence, starting from $\mathcal{N}$, obtained using canonical transformations, one can prove that the minimal normal form $\mathcal{N}_{\mathrm{MNF}}$ exists, and one can also derive the relationship between the invariant actions J and J_{MNF} of the two maps.

However, the above technique, if used to calculate the minimal normal form, requires that we first normalize the map using canonical transformations and *then* transform it further to the minimal normal form. The procedure outlined at the beginning of this section offers a method to calculate the minimal normal form *directly,* and so it will be employed below, in this paper.

It is not, at the present time, immediately obvious how to generalize the minimal normal form to higher phase-space dimensions. The difficulty arises because the tune-shift for μ_x, say, depends on both J_x and J_y, and so one cannot express $J_{x,\mathrm{MNF}}$ purely in terms of J_x, because J_y is necessarily involved. It has therefore been suggested [7] that the minimal normal form does not exist in higher phase-space dimensions. We believe that this is not necessarily the case, but rather that some further refinement of the concept may be required to generalize to more than two phase-space dimensions, possibly following the method of averaging described in Ref. [6] and utilizing the "multiple-phase" technique referred to in Ref. [10]. However, this is beyond the scope of the present paper.

C. Explicit solution for coefficients

The above rather terse description explains the basic aims of the minimal normal-form method, as applied to the evaluation of maps, and the sense in which it is "minimal." To elucidate the above concepts, (1) the explicit details of the calculation of the coefficients T_{pq} of the near-identity transformation, and also the amplitude-dependent tune-shift parameter μ', will now be given and (2) a worked example, viz., the Hénon map, will be treated below. A computer program has also been generated

to implement the general formalism in two dimensions of phase space, and will be used later in this paper to study a few model examples which are more typical in accelerator applications.

The procedure is as follows: First, Eqs. (2.12) and (2.13) are substituted into Eq. (2.10), and terms collected in powers of ϵ, to obtain

$$u_{n+1}+\sum_k \epsilon^k T_k(u_{n+1},u_{n+1}^*) = \lambda\left[u_n+\sum_k \epsilon^k T_k(u_n,u_n^*)\right]+\sum_k \epsilon^k N_k(u,u^*) , \tag{2.28}$$

with new homogeneous polynomials

$$N_k=\sum_{(p+q=k+1)} N_{pq}|p,q\rangle , \tag{2.29}$$

with the notation $|p,q\rangle = u^p u^{*q}$. This can be performed quite easily by a computer. We then put

$$u_{n+1}=\lambda u_n \exp(-i\epsilon^2\mu' u_n u_n^*) , \tag{2.30}$$

where $\mu'=i\tilde{U}_2/\lambda$, whence

$$\sum_{(p+q=k+1)} \epsilon^k T_{pq}(\lambda^{p-q}-\lambda)|p,q\rangle = \sum_{(p+q=k+1)} \epsilon^k N_{pq}|p,q\rangle - \sum_{\substack{(p+q=k+1)\\(r\geq 1)}} \epsilon^k \lambda^{p-q} T_{p-rq-r} \times \frac{[-i\mu'(p-q)]^r}{r!}|p,q\rangle . \tag{2.31}$$

It is now apparent why the coefficients T_{pq}, with $p=q+1$, cannot be determined by this procedure alone: their coefficient on the left-hand side (lhs) vanishes, since $\lambda^{p-q}-\lambda=0$ for such terms. Hence this leaves resonant monimials $|p+1,p\rangle$ on the right-hand side (rhs), i.e., the coefficients $\tilde{U}_{2p}$. The solution for T_{pq}, except for the free terms, is thus

$$T_{pq}=\frac{1}{\lambda^{p-q}-\lambda}\times\left[N_{pq}-\lambda^{p-q}\sum_{r\,(\geq 1)} T_{p-rq-r}\times\frac{[-i\mu'(p-q)]^r}{r!}\right] , \tag{2.32}$$

and the tune-shift coefficients are given by

$$\tilde{U}_{2k}=N_{k+1k}-\lambda\sum_{r\,(\geq 1)} T_{k+1-rk-r}\frac{(-i\mu')^r}{r!} . \tag{2.33}$$

It is understood that the sum over r terminates when the indices reach zero or negative values. Formally, all such T_{p-rq-r} are set to zero. The free functions are determined by requiring that the terms in the series expansion for the equation for u_{n+1} add up to a single complex exponential $\exp(-i\epsilon^2\mu' u_n u_n^*)$.

We note the following caveat: if the $O(\epsilon^2)$ tune shift vanishes, so that the lowest-order nonzero tune shift is $-i\epsilon^4\mu''(u_n u_n^*)^2$, then the free functions should be chosen so that the equation for u_n has the form

$$u_{n+1}=\lambda u_n \exp(-i\epsilon^4\mu'' u_n^2 u_n^{*2}) . \tag{2.34}$$

The formalism to handle this situation will not be developed in detail in this paper, but should be included in a more complete development of the minimal normal-form method. A numerical example will be studied below to indicate the consequences of a vanishing, or small, $O(\epsilon^2)$ tune shift parameter.

D. Hénon map

To clarify the above abstract formulas, we shall now work through an example with a simple but nontrivial nonlinearity, viz., the Hénon map [11],

$$\begin{bmatrix}x\\p\end{bmatrix}_{n+1}=\begin{bmatrix}\cos\mu & \sin\mu\\ -\sin\mu & \cos\mu\end{bmatrix}\begin{bmatrix}x\\p+\epsilon x^2\end{bmatrix}_n . \tag{2.35}$$

The notation has already been defined above. In terms of $z=x+ip$ and $\lambda=e^{-i\mu}$, the equation for the map is

$$z_{n+1}=\lambda z_n+\frac{i\epsilon\lambda}{4}(z_n+z_n^*)^2 . \tag{2.36}$$

To $O(\epsilon)$, the near-identity transformation to the normal-form variable u is only $z\simeq u+\epsilon T_1$; hence,

$$u_{n+1}+\epsilon T_1(u_{n+1},u_{n+1}^*) \simeq \lambda[u+\epsilon T_1(u_n,u_n^*)]+\frac{i\epsilon\lambda}{4}(u_n+u_n^*)^2 . \tag{2.37}$$

To this order of approximation, one can put $u_{n+1}=\lambda u_n$ in the argument of T_1 on the lhs, which yields

$$u_{n+1}=\lambda u_n+\epsilon[T_{20}(\lambda-\lambda^2)u_n^2+T_{11}(\lambda-1)u_n u_n^* + T_{02}(\lambda-\lambda^{*2})u_n^{*2}]+\frac{i\epsilon\lambda}{4}(u_n+u_n^*)^2 . \tag{2.38}$$

Equating terms of $O(\epsilon)$ yields the solutions

$$T_{20}=\frac{i}{4}\frac{1}{\lambda-1}\ ,$$
$$T_{11}=-\frac{i}{2}\frac{\lambda}{\lambda-1}\ , \tag{2.39}$$
$$T_{02}=-\frac{i}{4}\frac{\lambda^3}{\lambda^3-1}\ .$$

The equation of motion for u_n will thus have no term of $O(\epsilon)$, i.e., $u_{n+1}=\lambda u_n+O(\epsilon^2)$. At the next order, $z\simeq u+\epsilon T_1+\epsilon^2 T_2$. This yields the relation

$$u_{n+1}+\epsilon^2 T_2(\lambda u_n,\lambda^* u_n^*)=\lambda[u+\epsilon^2 T_2(u_n,u_n^*)]+\frac{i\epsilon^2\lambda}{2}(u_n+u_n^*)(T_1+T_1^*)\ . \tag{2.40}$$

Collecting together the terms up to $O(\epsilon^2)$,

$$\begin{aligned}u_{n+1}+\epsilon^2[(\lambda^3-\lambda)T_{30}u^3+(\lambda-\lambda)T_{21}u^2u^*+(\lambda^*-\lambda)T_{12}uu^{*2}+(\lambda^{*3}-\lambda)T_{03}u^{*3}]\\ =\lambda u_n+\frac{i\epsilon^2\lambda}{2}[u^3(T_{20}+T_{02}^*)+u^2u^*(T_{11}+T_{11}^*+T_{20}+T_{02}^*)\\ +uu^{*2}(T_{02}+T_{20}^*+T_{11}+T_{11}^*)+u^{*3}(T_{02}+T_{20}^*)]\ .\end{aligned} \tag{2.41}$$

This determines T_{30}, T_{12}, and T_{03}, but not T_{21}, because its coefficient vanishes, and the term in u^2u^* cannot be eliminated on the rhs: it contributes to $\tilde{U}_2$ or $-i\mu'$. The expression for $\tilde{U}_2$ is, from above,

$$\tilde{U}_2=\frac{i\lambda}{2}(T_{11}+T_{11}^*+T_{20}+T_{02}^*)\ , \tag{2.42}$$

and so the tune-shift parameter is given by

$$\begin{aligned}\mu'=i\frac{\tilde{U}_2}{\lambda}&=-\frac{i}{2}\left[-\frac{1}{2}\frac{\lambda}{\lambda-1}+\frac{1}{2}\frac{\lambda^*}{\lambda^*-1}\right.\\ &\quad\left.+\frac{1}{4}\frac{1}{\lambda-1}+\frac{1}{4}\frac{\lambda^{*3}}{\lambda^{*3}-1}\right]\\ &=\frac{i}{8}\frac{2\lambda^3+3\lambda^2+3\lambda+2}{\lambda^3-1}\ .\end{aligned} \tag{2.43}$$

We notice that the rhs diverges if $\lambda=1$ or $e^{\pm i2\pi/3}$, i.e., the well-known integer and third-integer resonances. The denominator of the next term in the tune shift will contain λ^5-1, etc. Using the property $\lambda^*=1/\lambda$, it is straightforward to verify that μ' is real. The next term in the normal-form equation of motion is

$$\begin{aligned}\tilde{U}_4=\frac{i\lambda}{2}[&T_{22}+T_{22}^*+T_{31}+T_{13}^*\\ &+(T_{20}+T_{02}^*)(T_{12}+T_{21}^*)\\ &+(T_{11}+T_{11}^*)(T_{21}+T_{12}^*)\\ &+(T_{02}+T_{20}^*)(T_{30}+T_{03}^*)+2\mu' T_{21}]\ .\end{aligned} \tag{2.44}$$

The derivation of the above result involves some tedious algebra, and is best handled by computer. The interested reader can consult Ref. [12]. As stated above, the as-yet-undetermined free function T_{21} appears in the expression for $\tilde{U}_4$, so it is now set by requiring that $\tilde{U}_4/\lambda=-\mu'^2/2$. At higher orders, T_{kk-1} is set by requiring that $\tilde{U}_{2k}/\lambda$ equal $(-i\mu')^k/k!$, for $k=2,3,4,\ldots$.

The implementation of the above calculations, for arbitrary maps, has been incorporated into a computer program, which will be used below to study various model systems. The program in fact employs a rudimentary version of the powerful differential algebra techniques [13], although such a fact is not relevant for our purposes here. A later paper will describe a fuller coupling of the present work with a differential algebra package.

III. NUMERICAL RESULTS

A. Differential equations

Although we are principally concerned with the study of discrete maps, our investigation of numerical models will commence by applying the minimal normal-form method to differential equations. There are various reasons for this, one of which is that first integrals of the motion (the energy, in particular) exist for the latter. Hence, one has an easily identifiable criterion for an error analysis, to check the accuracy of the various approximations to the exact solution. We select for study two well-known equations, viz., a quadratic and a cubic nonlinearity (Duffing oscillator), i.e.,

$$\dot{z}=-i\mu z+\frac{i\epsilon}{4}(z+z^*)^2 \tag{3.1}$$

and

$$\dot{z}=-i\mu z+\frac{i\epsilon^2}{8}(z+z^*)^3\ , \tag{3.2}$$

and then the sum and difference of the two perturbations, i.e.,

$$\dot{z}=-i\mu z+\frac{i\epsilon}{4}(z+z^*)^2\pm\frac{i\epsilon^2}{8}(z+z^*)^3\ . \tag{3.3}$$

We may set $\mu=1$ without loss of generality. The phase-space trajectories for the first two equations of motion above are shown in Fig. 1. The domain of stable orbits around the origin are clearly identifiable. The above graphs have been plotted using $\epsilon=1$; the value of ϵ merely determines the location of the separatrix, and has been chosen so that $z_0=1$ is a fixed point in both cases.

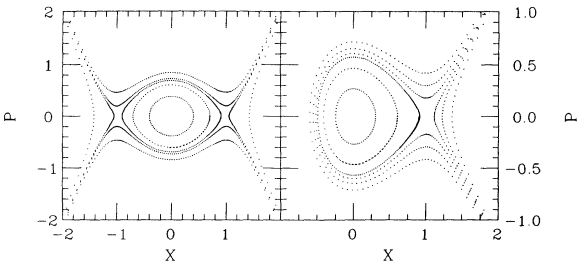

FIG. 1. Phase-space trajectories for a cubic nonlinearity (Duffing oscillator) on the left, and a quadratic nonlinearity on the right, calculated using a symplectic integrator.

The solution for the coefficients T_{pq} in the normal-form transformation, in the case of differential equations, is almost the same as that for maps, and a derivation very similar to that of Eq. (2.32) yields

$$T_{pq}=\frac{i}{(p-q-1)\mu}[N_{pq}+i(p-q)\mu' T_{p-1q-1}] \ . \tag{3.4}$$

The free terms, for which $p=q+1$, are set by requiring that the $\tilde{U}_{2k}$ vanish for $k\geq 2$ in Eq. (2.6), in the case of the minimal normal form, or by requiring that $\tilde{P}_{2k}=0$ for $k\geq 1$, in the case of a canonical transformation.

Equation (3.2) will be treated first, because the calculations of the amplitude-dependent tune shift, etc., are simpler for a cubic rather than a quadratic nonlinearity. Three methods of solution were used: (1) set all free functions to zero (the "$F=0$" choice), (2) a canonical transformation (denoted CT below), and (3) the minimal normal form (denoted MNF). For this perturbation, the $O(\epsilon^2)$ tune-shift parameter can be read off immediately and is

$$\mu'=-\tfrac{3}{8} \tag{3.5}$$

for all of the above methods. It is only at higher orders that the tune-shift parameters, etc., differ among the methods.

To examine the convergence of the series expansions of the various methods above, D'Alembert's test of convergence [14] suggests that we plot the magnitudes of the kth-order terms $|T_k|$, or $\log_{10}|T_k|$, as a function of k. Since T_k is actually a polynomial with several terms, the function actually plotted was

$$\log_{10}\left[\sum_{i+j=k+1}|T_{ij}|\right] ,$$

i.e., the sum of the magnitudes of the coefficients of the individual terms in each T_k. The results are shown in Fig. 2, where the curves corresponding to the various choices are labeled $F=0$, CT, or MNF, respectively. It is striking that the coefficients from the first two methods ($F=0$ and CT) do not decrease with the order at all, whereas those calculated using the MNF method decrease rapidly. This is equivalent to saying that the minimal normal form achieves, at low orders of perturbation theory, a better approximation to the exact solution, thus requiring smaller higher-order corrections.

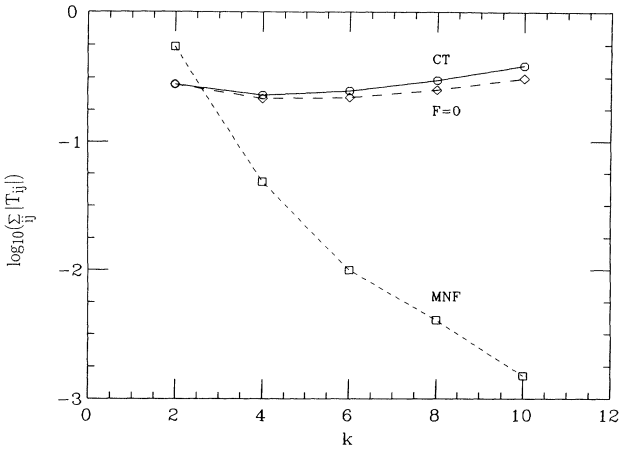

FIG. 2. Graph of the magnitudes of the coefficients in the normal-form transformation as a function of the order of perturbation theory, for various methods of choosing the free functions for a Duffing oscillator. MNF denotes minimum normal form and CT denotes canonical transformation methods.

Other relevant functions to examine and compare among the methods are the free functions T_{k+1k}, the tune-shift coefficients $\tilde{U}_{2k}$, and the Poisson bracket coefficients $\tilde{P}_{2k}$. Table I offers a comparison of the values of these coefficients. For the $F=0$ choice, the values of $\tilde{U}_{2k}/\lambda$ and $\tilde{P}_{2k}$ are tabulated. The free functions are omitted, since they are all zero. For the CT, the values of T_{k+1k} and $\tilde{U}_{2k}/\lambda$ are presented, while for the MNF, the values of T_{k+1k} and $\tilde{P}_{2k}$ are given. It is evident that for both the $F=0$ and the CT methods, the values of the tabulated coefficients initially decrease slightly, but soon turn around and start to increase with the order, e.g., the tune-shift corrections $\tilde{U}_{2k}/\lambda$. The MNF method, on the other hand, yields terms that decrease rapidly with the order.

An important test of the accuracy of the various perturbative solutions is to compute the value of the energy. Since the equation of motion is autonomous, the energy should remain constant as a function of time. In general, the value of any first integral of the motion should be computed and checked for constancy as a function of time. For the Duffing oscillator of Eq. (3.2), the energy is

$$E=\frac{\mu}{2}(p^2+x^2)-\frac{\epsilon^2 x^4}{4} \ . \tag{3.6}$$

In our analysis, $\mu=\epsilon=1$. The amplitude was set at $\rho\simeq 0.5$, so as to be well within the separatrix, so that all the methods would converge rapidly. For each method, the calculations were performed to $O(\epsilon^4)$ and $O(\epsilon^6)$, i.e., the near-identity transformation to the normal form was calculated through T_4 or T_6, respectively, and the tune shifts were also calculated through $O(\epsilon^4)$ or $O(\epsilon^6)$, for the $F=0$ and CT cases. For the MNF, the tune shift terminated at $O(\epsilon^2)$, of course. The value of the relative error $(E-E_0)/E_0$, where E_0 is the initial energy, is plotted against the time in Fig. 3. A total of six curves are shown and labeled, viz., dashes for the MNF, solid for the CT,

TABLE I. Values of the free functions, tune-shift coefficients, and Poisson-bracket coefficients for the various methods of calculating the normal form for a map with a thin-lens octupole.

	Zero-free functions		Canonical transformation		Minimal normal form	
k	$\tilde{U}_{2k}/\lambda$	$\tilde{P}_{2k}$	T_{k+1k}	$\tilde{U}_{2k}/\lambda$	T_{k+1k}	$\tilde{P}_{2k}$
1	0.375	0	0	0.375	−0.265 625	−1.062 5
2	0.1992	−0.0791	0.0131	0.1992	0.015 991	0.228 515
3	0.1732	−0.1296	0.0162	0.1831	0.001 272	0.014 648
4	0.1812	−0.1844	0.0194	0.2038	0.000 169	0.007 305
5	0.2092	−0.2535	0.0239	0.2504	−0.000 031	0.002 941
6	0.2570	−0.3447	0.0303	0.3267	−0.000 046	0.000 860

and crosses for the $F=0$ choice. The results for the $F=0$ and CT methods are very similar, but that for the MNF method is quite clearly better than both. Even at $O(\epsilon^4)$, the MNF yields an error comparable to that from the others at $O(\epsilon^6)$, while when the MNF is used to $O(\epsilon^6)$, the error is almost invisible on the scale of Fig. 3.

On the above evidence, the minimal normal form appears to be a good choice when utilizing the freedom in setting up the near-identity transformation to the normal form, but more evidence is required, using other equations of motion. The next model treated was Eq. (3.1), which has a quadratic nonlinearity. For this equation, two orders of perturbation theory are required to derive the amplitude-dependent tune shift, and the coefficient is

$$\mu' = -\frac{5}{12\mu} . \tag{3.7}$$

As explained above, this value is the same for all three formalisms. Analogous to Table I, the values of the free functions T_{k+1k}, the tune-shift coefficients $\tilde{U}_{2k}/\lambda$, and the Poisson-bracket coefficients $\tilde{P}_{2k}$ are listed in Table II. The results are, if anything, even more impressive than those for the Duffing oscillator. Indeed, both the $F=0$ and CT methods yielded coefficients T_{ij} whose magnitudes *increased* with the order k, while the MNF yields terms that *decreased*. A graph of the magnitudes of the coefficients

$$\log_{10}\left[\sum_{i+j=k+1} |T_{ij}|\right]$$

as a function of the order k also confirmed that the MNF coefficients are several orders of magnitude smaller than those from the other methods.

However, there are cases where the use of the minimal normal form as described above is not so effective. Note, from Eq. (2.25), that if μ' is small, or vanishes, then the minimal normal form does not exist. In the present formalism, the free functions would diverge when attempting to cancel out the tune-shift terms. For example, for the potential

$$V = -\tfrac{8}{25}\epsilon x^3 + \frac{\epsilon^2 x^4}{4} , \tag{3.8}$$

with $\mu=\epsilon=1$, the tune-shift parameter is $\mu' \simeq -0.009$, i.e., almost zero. The corresponding graph to Fig. 2 was plotted, in Fig. 4. The MNF coefficients, this time, were larger than those from the $F=0$ and CT methods, which were not directly dependent on the value of μ'.

There is, however, a "cure" for this problem. Recall that it was pointed out above that if $\mu'=0$, then the MNF prescription should be modified to retain the $O(\epsilon^4)$ tune-shift parameter μ'', and to use the free functions to cancel the higher-order tune-shift terms, i.e., to use T_{21} to cancel $\tilde{U}_6$, and T_{32} to cancel $\tilde{U}_8$, etc. Using the free functions in this way, i.e., keeping both μ' and μ'' nonzero, and going up four orders to set the value of each free function, the minimal normal-form method was applied to the above potential again. The values of the higher-order tune-shift parameters were actually not zero, but small, because the full implementation of the MNF prescription for this situation required the solution of quadratic equations; hence, the free functions were only set approximately. More detailed results, using a more sophisticated computer program, will be presented elsewhere. The values of the two lowest-order tune-shift parameters were $\mu' \simeq -0.009$ and $\mu'' \simeq 0.533$, i.e., μ'' was not close to zero. The magnitudes of the coefficients in the series expansion are shown in Fig. 5, together with the previously derived solutions for the $F=0$ and CT methods, which are unchanged from Fig. 4. The MNF coefficients are now an order of magnitude *smaller* than those from the $F=0$ and CT methods, instead of eight or-

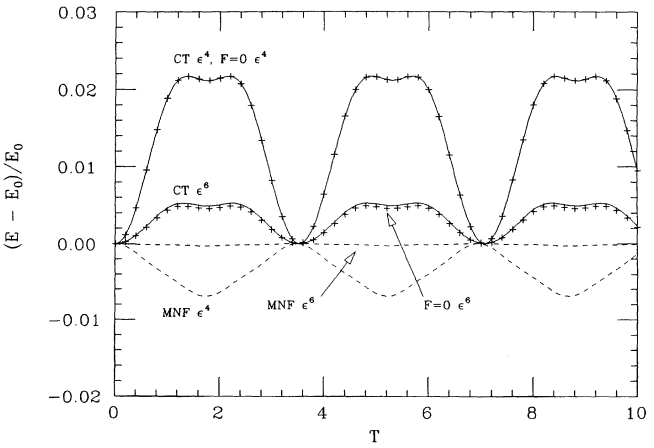

FIG. 3. Graph of the relative error $(E-E_0)/E_0$ in the energy as a function of time, for calculations through fourth and sixth order, for various methods of performing the normal-form transformation. The equation of motion contains a cubic nonlinear term.

TABLE II. Values of the free functions, tune-shift coefficients, and Poisson-bracket coefficients for the various methods of calculating the normal form for a map with a thin-lens sextupole.

	Zero-free functions		Canonical transformation		Minimal normal form	
k	$\tilde{U}_{2k}/\lambda$	$\tilde{P}_{2k}$	T_{k+1k}	$\tilde{U}_{2k}/\lambda$	T_{k+1k}	$\tilde{P}_{2k}$
1	0.4166	0.2222	−0.0555	0.4166	−0.545 138	−1.958 333
2	0.4542	0.5666	−0.0836	0.4079	0.092 562	1.286 747
3	0.7896	1.6911	−0.1669	0.6202	−0.012 415	−0.326 260
4	1.6569	5.1819	−0.3599	1.1148	−0.004 003	0.044 213
5	3.8537	16.0340	−0.8056	2.1898	−0.001 471	0.000 397
6	9.5641	49.9176	−1.8464	4.5448	−0.000 344	−0.002 380

ders of magnitude larger, as in Fig. 4. The improvement in the MNF results is dramatic.

Hence, we may conclude that the minimal normal form has the potential to be a good method of exploiting the freedom available in the transformation from the original phase-space coordinates to the normal form. It holds out the promise of offering a good approximation to the exact solution using only low orders of perturbation theory, thereby requiring smaller higher-order corrections than other methods such as a canonical transformation. However, it was also shown that the basic implementation of the method, as described in this paper, could yield worse results than other methods, if the magnitude of the lowest-order tune-shift parameter u' was small, or zero. In that case, it was shown that the appropriate step was to retain higher-order tune-shift parameters, e.g., μ'', in the equation of motion for the normal form. The minimal normal-form method then again yielded better results than the other methods studied in the tests above. Hence, some judgment is required by the user as to how many tune-shift coefficients should be retained to nonzero values before using the free functions to cancel the rest. The merit of the minimal normal-form method for discrete maps will now be investigated.

B. Discrete maps

The calculations of the expressions for the normal form for discrete maps are similar to those for differential equations, but there is no longer an easily identifiable first integral of the motion, to provide a convenient basis for an error analysis. Hence, the analysis below will be restricted to an examination of the behavior of the growth of the magnitudes of the coefficients in the transformation to the normal form, as a function of the order of perturbation theory. The three choices for the normal form will again be denoted $F=0$, CT, and MNF. The maps treated below used a single thin-lens sextupole or octupole, i.e., a quadratic or cubic nonlinearity. A plot of the phase-space trajectories for these maps is shown in Fig. 6. The tunes were set to $\nu=0.255$ and 0.34, respectively, where $\mu=2\pi\nu$, and the value of ϵ was chosen so that the separatrices would be at $x^2+p^2\simeq 1$ in both cases. This leads to the choices $\epsilon=0.2$ and 0.1, respectively. For the octupole, the map equation is

$$z_{n+1}=\lambda z_n+\frac{i\epsilon^2\lambda}{8}(z_n+z_n^*)^3 \ . \tag{3.9}$$

The sextupole map would normally be very similar,

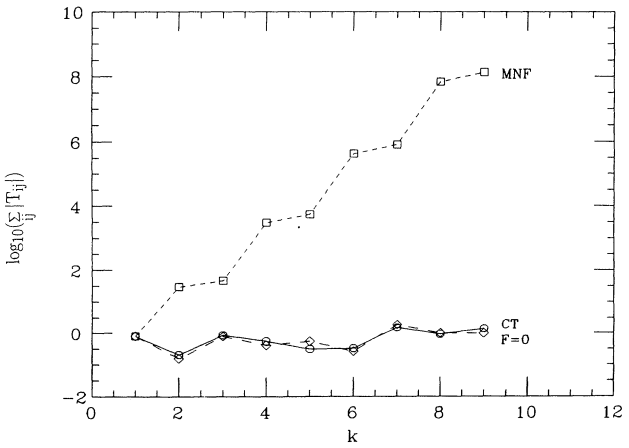

FIG. 4. Graph of the magnitudes of the coefficients in the normal-form transformation as a function of the order of perturbation theory, with quadratic and cubic nonlinear terms chosen so as to yield a small second-order tune-shift parameter.

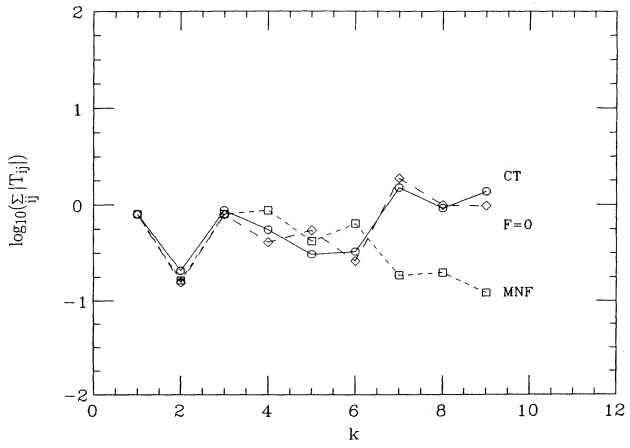

FIG. 5. Graph of the magnitudes of the coefficients in the normal-form transformation as a function of the order of perturbation theory. Both the second- and fourth-order tune-shift parameters were retained in the minimal normal-form method.

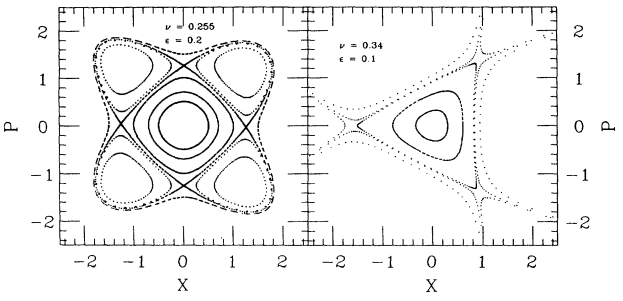

FIG. 6. Phase-space trajectories for maps with a thin-lens octupole (left) and sextupole (right). The tunes are labeled in each figure. The nonlinear multipole strength is chosen to place the separatrix at $x^2+p^2\simeq 1$ in each case.

$$z_{n+1}=\lambda z_n+\frac{i\epsilon\lambda}{4}(z_n+z_n^*)^2 , \tag{3.10}$$

i.e., the Hénon map. For aesthetic reasons, however, to create phase-space trajectories symmetric around the x axis, the sextupole was located diametrically opposite the observation point, leading to the map equation

$$z_{n+1}=\lambda z_n+\frac{i\epsilon\sqrt{\lambda}}{4}(\sqrt{\lambda}z_n+\sqrt{\lambda^*}z_n^*)^2 , \tag{3.11}$$

which was used to generate Fig. 6. It has been verified that the location of the sextupole made no difference to the convergence of the series expansion for the normal form. The values of the $O(\epsilon^2)$ tune-shift parameter are

$$\mu'=-\tfrac{3}{8} , \tag{3.12}$$

for the thin-lens octupole kick in Eq. (3.9), and

$$\mu'=\frac{i}{8}\frac{2\lambda^3+3\lambda^2+3\lambda+2}{\lambda^3-1} , \tag{3.13}$$

for the thin-lens sextupole kick in Eq. (3.11), i.e., the same as the Hénon map.

As explained above, in accordance with D'Alembert's test of convergence [14], the various methods for calculating the normal form were compared by plotting the function

$$\log_{10}\left[\sum_{i+j=k+1}|T_{ij}|\right]$$

against the order k. The results for the thin-lens octupole map, Eq. (3.9), with a tune of $\nu=0.255$, are shown in Fig. 7. The results from all three methods are almost the same, and although the MNF result is smaller than the others, the difference is slight. It is not immediately clear why this is so; perhaps it may be due to the presence of a small denominator in the coefficients, caused by the location of large low-order resonance islands close to the origin. In an attempt to approximate the conditions of the differential equations, the calculation was repeated using a tune of $\nu=0.01$, i.e., a small phase advance per turn. The results are shown in Fig. 8. The MNF result, this time, is distinctly better than the others, the coefficients being smaller by two orders of magnitude at the tenth order.

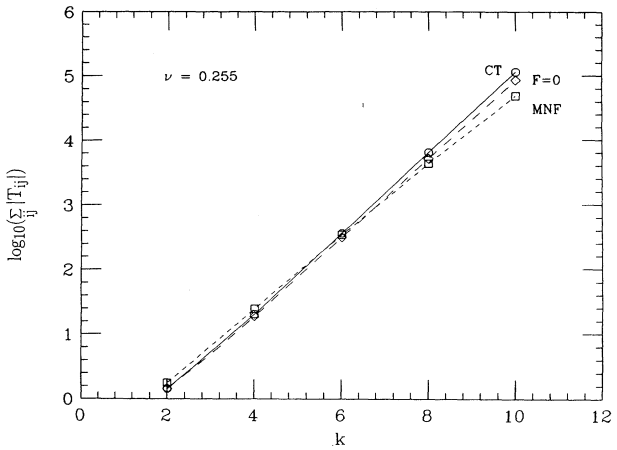

FIG. 7. Graph of the magnitudes of the coefficients in the normal-form transformation as a function of the order of perturbation theory, for various methods of choosing the free functions, for a map with a single thin-lens octupole, using a tune of $\nu=0.255$.

To examine the behavior for a different map, the thin-lens sextupole map of Eq. (3.11) was studied next. The results are shown in Fig. 9, for a tune of $\nu=0.34$. This time, the MNF coefficients for the normal form are clearly smaller than those from the $F=0$ and CT methods. Use of a combined sextupole-octupole kick, viz.,

$$z_{n+1}=\lambda z_n+\frac{i\epsilon\lambda}{4}(z_n+z_n^*)^2\pm\frac{i\epsilon^2\lambda}{8}(z_n+z_n^*)^3 , \tag{3.14}$$

with a tune of $\nu=0.255$, again yielded results which were almost the same for all three methods.

A lattice of thin-lens focusing-defocusing (FODO) cells was now constructed, to provide an example of a model closer to actual accelerator applications. A block dia-

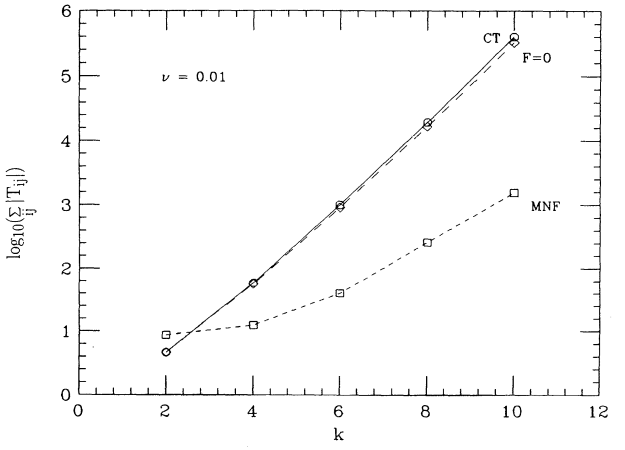

FIG. 8. Graph of the magnitudes of the coefficients in the normal-form transformation as a function of the order of perturbation theory, for various methods of choosing the free functions, for a map with a single thin-lens octupole. The small-amplitude tune is $\nu=0.01$.

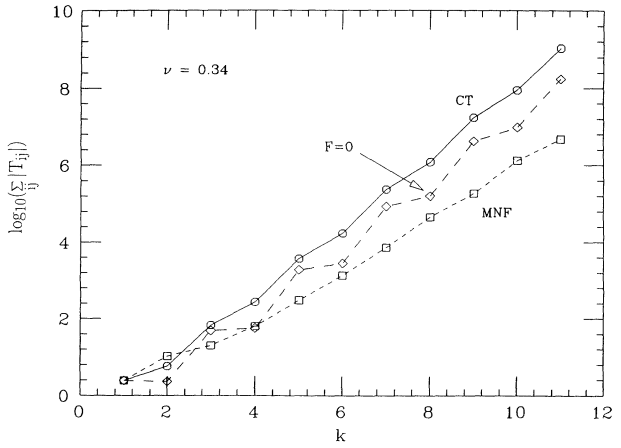

FIG. 9. Graph of the magnitudes of the coefficients in the normal-form transformation as a function of the order of perturbation theory, for various methods of choosing the free functions, for a map with a single thin-lens sextupole. The small-amplitude tune is $\nu=0.34$.

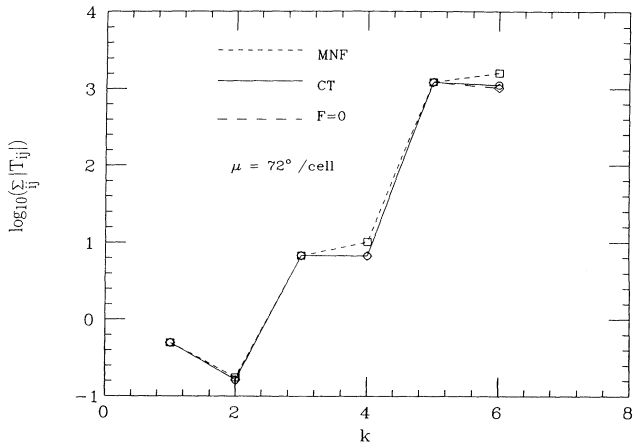

FIG. 11. Graph of the magnitudes of the coefficients in the normal-form transformation as a function of the order of perturbation theory, for a lattice of 24 thin-lens FODO cells with two sextupoles per cell. The phase advance per cell is $\mu \simeq 72°$.

gram of one cell is shown in Fig. 10. The cell half-length was $l=4.2$ m, and the quadrupole inverse focal lengths were $k_f=-k_d=0.28$ m^{-1}, leading to a betatron phase advance of approximately 72° across the cell. The above parameter values are based on those of the AGS Booster at Brookhaven National Laboratory [15] (BNL), which has 24 cells and an operating tune of between 4.8 and 5. The origin and end of the cell were located at the center of a focusing quadrupole to make the end points symmetry points of the lattice. The sextupole kicks were given by $\Delta x'=-\epsilon s_{f,d}x^2$, with $s_f=-s_d=0.05$ m^{-2}. A computer program was used to calculate the Taylor expansion of the one-turn map around the phase-space origin, and to diagonalize the linear motion, to yield a series in the form Eq. (2.10). The amplitudes of the coefficients in the normal-form transformation were plotted against the order of the expansion in Fig. 11. The results from all three methods are very similar. Note that, in all three cases, the coefficients decreased in magnitude until a small denominator was reached (because a tune of 4.8 is close to a $\frac{1}{5}$ resonance), after which the magnitudes increased.

Hence, the minimal normal-form method, when applied to discrete maps, sometimes yields better results

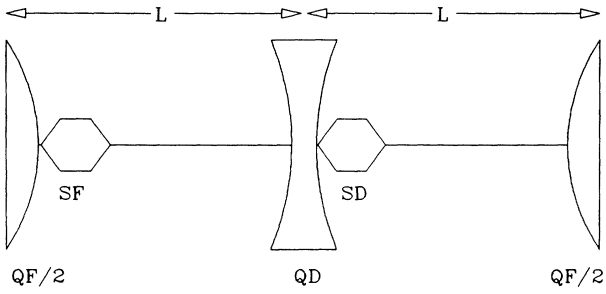

FIG. 10. Block diagram of thin-lens FODO cell with nonlinear elements (sextupoles) placed next to each quadrupole.

than other methods, but the difference is not as pronounced as when solving differential equations. In all of the maps studied above, the free functions were chosen to cancel the higher-order tune-shift coefficients beyond $O(\epsilon^2)$. However, in those cases where the minimal normal-form results were not better than those from other methods, it may be a good idea to retain both the $O(\epsilon^2)$ and $O(\epsilon^4)$ tune-shift terms, and to use the free functions to cancel the coefficients starting at $O(\epsilon^6)$, based on the experience with differential equations above. This requires a more sophisticated formalism and computer program, because the equations to be solved are not as straightforward. Future reports will address the results from such a prescription.

IV. CONCLUSION

The method of normal forms has been reviewed and the superiority of the minimal normal-form method has been demonstrated for ordinary nonlinear autonomous differential equations. The minimal normal-form method has also been extended to treat discrete maps. The application to the evaluation of one-turn maps for accelerators yields mixed results; hence, the superiority of the minimal normal form is not as clearly visible. Further studies in investigating the effect of small denominators in the vicinity of low-order resonances will be attempted, to improve the convergence of the perturbation expansion. A differential algebra package of computer programs will be used to facilitate the numerical manipulations necessary for the applications.

A major application of the method presented here in the calculation of the one-turn map is to use the map to evaluate the effect of nonlinear perturbations on the lattice functions, such as betatron functions, the dispersion function, chromaticity, and tunes of the accelerator. If such improvements are proven to be possible, the minimal normal-form method can serve as a standard way of calculating lattice functions of an accelerator or storage ring.

ACKNOWLEDGMENTS

The authors would like to thank Professor P. Kahn and Professor Y. Zarmi for fruitful discussions on the method of minimal normal forms, and Mrs. D. Murray for help on part of the calculations. Discussions with D. Abell, P. Channel, J. Ellison, E. Forest, and A. Sessler are also appreciated. This work was supported in part by the U.S. Department of Energy.

[1] E. D. Courant and H. S. Snyder, Ann. Phys. (N.Y.) **3**, 1 (1958).
[2] E. Forest and K. Hirata, KEK Report No. 92-12, 1992 (unpublished). See also references therein.
[3] P. B. Kahn and Y. Zarmi, Physica D **54**, 65 (1991).
[4] G. Turchetti, in *Nonlinear Problems in Future Particle Accelerators,* edited by W Scandale and G. Turchetti (World Scientific, Singapore, 1991).
[5] W. Scandale, F. Schmidt, and E. Todesco, Part. Accel. **35**, 53 (1991).
[6] J. A. Ellison, A. W. Sáenz, and H. S. Dumas, J. Differ. Equations **84**, 383 (1990).
[7] E. Forest (private communication).
[8] A. J. Dragt and J. M. Finn, J. Math. Phys. **17**, 2215 (1976).
[9] A. J. Dragt and E. Forest, J. Math. Phys. **24**, 2734 (1983).
[10] P. Lochak and C. Meunier, *Multiphase Averaging for Classical Systems* (Springer-Verlag, New York, 1988).
[11] M. Hénon, in *Chaotic Behavior of Deterministic Systems,* edited by G. Iooss *et al.* (North-Holland, Amsterdam, 1983).
[12] S. R. Mane and W. T. Weng, Brookhaven National Laboratory AGS/AD/Tech Note No. 368, 1992 (unpublished).
[13] M. Berz, Nucl. Instrum. Methods A **298**, 473 (1990).
[14] I. S. Gradshteyn and I. M. Rhyzik, *Table of Integrals, Series, and Products,* 4th ed. (Academic, New York, 1980), p. 5.
[15] W. T. Weng, Part. Accel. **27**, 13 (1990).